Sub-Poissonian Number Differences in Four-Wave Mixing of Matter Waves

J.-C. Jaskula,[1] M. Bonneau,[1] G. B. Partridge,[1] V. Krachmalnicoff,[1,*] P. Deuar,[2] K. V. Kheruntsyan,[3] A. Aspect,[1] D. Boiron,[1] and C. I. Westbrook[1]

[1]*Laboratoire Charles Fabry de l'Institut d'Optique, CNRS, Univ Paris-Sud, Campus Polytechnique RD128 91127 Palaiseau, France*
[2]*Institute of Physics, Polish Academy of Sciences, Aleja Lotników 32/46, 02-668 Warsaw, Poland*
[3]*ARC Centre of Excellence for Quantum-Atom Optics, School of Mathematics and Physics, University of Queensland, Brisbane, Queensland 4072, Australia*

(Received 30 July 2010; published 2 November 2010)

We demonstrate sub-Poissonian number differences in four-wave mixing of Bose-Einstein condensates of metastable helium. The collision between two Bose-Einstein condensates produces a scattering halo populated by pairs of atoms of opposing velocities, which we divide into several symmetric zones. We show that the atom number difference for opposing zones has sub-Poissonian noise fluctuations, whereas that of nonopposing zones is well described by shot noise. The atom pairs produced in a dual number state are well adapted to sub–shot-noise interferometry and studies of Einstein-Podolsky-Rosen–type nonlocality tests.

DOI: 10.1103/PhysRevLett.105.190402 PACS numbers: 03.75.Nt, 34.50.Cx, 42.50.Dv

The creation of squeezed states of the electromagnetic field has been a major preoccupation of quantum optics for several decades [1]. Such states are not only inherently fascinating, but they also have the potential to improve sensitivity in interferometers [1], going beyond the ''shot noise'' or standard quantum limit. In the field of atom optics, workers are beginning to use the intrinsic nonlinearities present in a matter wave field to produce nonclassical states, especially squeezed states [2–7]. Indeed, an atom interferometer using squeezed inputs was recently demonstrated [8]. In our case, we produce dual number states in four-wave mixing of Bose-Einstein condensates (BECs). These states form the basis of a very different proposal for atom interferometry beyond the standard quantum limit [9–11]. Squeezing of atom samples may prove even more important than squeezing of light because the number of available atoms is often limited; therefore, surpassing the standard quantum limit can be the only way to increase the signal-to-noise ratio and improve performance. In interferometry proposals relying on dual number states, the observable corresponding to the relative phase is completely undetermined. Paradoxically, after passing through a beam splitter, the phase difference is no longer undetermined, but is peaked with a dispersion below the shot noise [10,11]. It has been argued that such states can be more robust to loss processes than maximally entangled states [10]. The pairs we produce should also be entangled in a sense analogous to [12]. A potentially interesting feature of our situation is that the pairs have large spatial separations (several cm here) and are thus well suited to investigations of (nonlocal) EPR entanglement [13] and Bell's inequalities using atoms.

Correlated photon pairs can be generated using optical processes such as four-wave mixing [14] or parametric down-conversion [15]. The matter wave analogs of these processes have recently been demonstrated [16,17]. The spontaneous four-wave mixing process [17], which we use here, simply corresponds to the collision of two Bose-Einstein condensates during which binary collisions produce scattered pairs of atoms with correlated momenta. Correlations, however, do not guarantee relative number squeezing (see Ref. [18] for an example) nor entanglement. The success of proposals such as those of Refs. [9–11] will likely be determined by the degree of squeezing. Thus, with a view towards using such correlated states in interferometry, it is important to verify that these processes do indeed produce squeezing. In this Letter, we demonstrate and quantify sub-Poissonian number differences produced in this process. Although the observation is not strictly sufficient to demonstrate squeezing in the sense of measuring fluctuations in two conjugate variables, we will often use the term squeezing below because the situation is a close atomic analog to experiments such as Ref. [19] in which relative intensity squeezing was observed in the generation of twin light beams created by parametric down-conversion.

We use metastable helium atoms which are detected by a micro-channel plate detector with a delay line anode [20]. The detector allows three-dimensional reconstruction of the momentum of each atom. Atoms in the 2^3S_1, $m_x = 1$ state are evaporatively cooled in a vertically elongated optical trap to produce a BEC with about 10^5 atoms and no discernible thermal component [21]. The use of an optical trap has resulted in substantially better shot to shot reproducibility than its magnetic antecedent [17]. The atomic angular momentum, which is due entirely to the electron spin, is defined relative to a 4 G magnetic holding field in the x direction (orthogonal to the optical trap axis). After cooling, the atomic spin is rotated away from the axis of the holding field by $\pi/2$ using a 2 ms rf

sweep [21]. The laser trap is then switched off and 1 μs later the condensate is split by applying counterpropagating laser beams for 2.5 μs. These beams are blue detuned from the 2^3P_0 state by 600 MHz, inclined at a 7° angle to the vertical axis and linearly polarized along the quantization axis. About one-third of the atoms are diffracted into each of two momentum classes traveling at $\pm 2v_{\mathrm{rec}}$, where $v_{\mathrm{rec}} = 9.2$ cm/s is the recoil velocity. Most of the rest remain at zero velocity. Binary collisions take place between atoms of all three velocity classes producing three collision halos with center of mass velocities $\pm v_{\mathrm{rec}}$ and zero. Since the atomic spin is orthogonal to the local field, 50% of the atoms are in the $m_x = 0$ state with respect to the magnetic field axis [21], and these atoms fall to the detector, unperturbed by magnetic field gradients. The trajectories of atoms in the $m_x = \pm 1$ states are perturbed by residual field gradients, and we therefore apply an additional gradient that causes these atoms to miss the detector entirely. The analysis is only focused on the collision halo centered at $+v_{\mathrm{rec}}$ [see Fig. 1(a)].

The collision halo centered at $v = 0$ has a radius $2v_{\mathrm{rec}}$ and is too large to be entirely captured by the detector while the two halos centered at $\pm v_{\mathrm{rec}}$, with radii v_{rec}, are entirely detected. In addition to binary scattering events, these two latter halos can be populated by spontaneous photon scattering whenever an atom at $v = 0$ scatters a photon from one of the diffraction laser beams. The diffraction efficiency depends on the product $I_1 I_2$ of the two laser intensities, while the spontaneous scattering into a given halo depends on only one of these intensities. So to reduce this effect we introduce an intensity imbalance in the two laser beams such that the halo centered at $+v_{\mathrm{rec}}$ is populated by the weaker beam and contains fewer such optically scattered atoms.

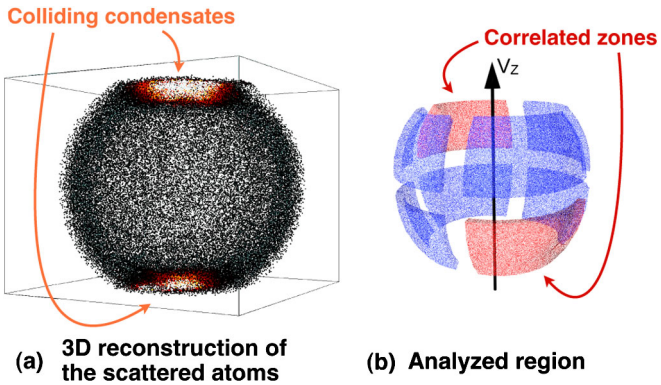

FIG. 1 (color online). View of the halo after the collision of two BECs and a subsequent ballistic expansion. (a) The experimental data plotted in momentum space, with each dot corresponding to a detected atom. Atoms on the collision halo are black, while the colliding, pancake-shaped BECs at the top and the bottom of the halo are orange/yellow. The collision axis v_z and the optical trap axis are both almost vertical. (b) Schematic view of the analyzed part ($|v_z| < 0.5v_{\mathrm{rec}}$) of the collision halo. Here we use $N_Z = 8$ zones that are separated from each other for better visualization. An example of two correlated zones is shown (red arrows). The number difference between these two zones shows sub–shot-noise fluctuations.

If squeezing is present, we expect a sub–shot-noise variance in the number difference of any two diametrically opposed volumes in the scattering halo [22]. For any other pair of volumes, we expect a variance corresponding to shot noise. We define the halo as a spherical shell of radius v_{rec} and thickness $\pm 0.15v_{\mathrm{rec}}$. The results are only weakly sensitive to this thickness, but as defined, it includes about 95% of the scattered atoms. We remove the areas on the halo containing the scattered BECs. The excised regions correspond to vertical velocities $|v_z| > 0.5v_{\mathrm{rec}}$. We divide the remainder of the halo in half at the equator and then make p vertical cuts along the meridians, dividing the halo into $N_Z = 4p$ equal zones, as shown in Fig. 1(b) for $p = 2$. We define a normalized number difference variance for zones i and j:

$$V_{i,j} = \frac{\langle (N_i - N_j)^2 \rangle - \langle N_i - N_j \rangle^2}{\langle N_i \rangle + \langle N_j \rangle}. \quad (1)$$

The brackets $\langle \ldots \rangle$ denote the average over the 3600 shots, and N_i refers to the number of atoms detected in the ith zone on a single shot. On average, we detect 150 atoms per shot on the whole analyzed region. If the zones i and j are uncorrelated, the normalized variance should be unity. Figure 2 shows the measured variances of all possible pairs of zones when the halo is cut into 16 zones. The eight pairs of correlated zones indeed show sub-Poissonian number differences ($V < 1$), and the 112 pairs of uncorrelated zones do not.

Perfectly correlated pairs and perfect detection would result in a zero variance. This, however, is almost unattainable in practice because of various imperfections, the most

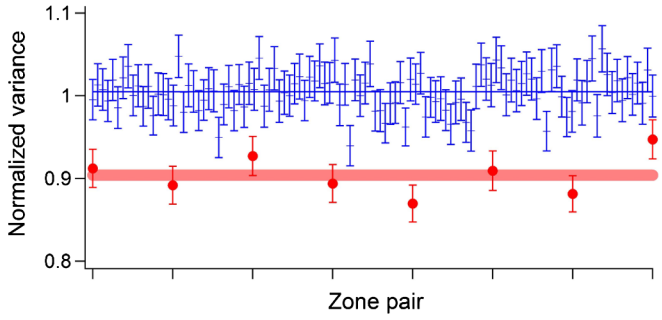

FIG. 2 (color online). Variance of all possible pairs of zones for the halo cut into 16 zones and summing $N_s = 3600$ shots. The normalized variance is $V_{i,j}$ and the error bars reflect its standard deviation $\delta V_{i,j}$ with $\delta V_{i,j}^2 = \frac{1}{N_s} \frac{\langle (N_i - N_j)^4 \rangle - \langle (N_i - N_j)^2 \rangle^2}{\langle N_i + N_j \rangle}$. Circles correspond to the eight correlated zones and crosses to the 112 uncorrelated ones. The two horizontal lines correspond to the mean of each data set with a thickness given by twice the standard deviation of the mean, considering each pair of zones as independent.

significant of which is the nonunit quantum efficiency η of our detector. The effect of the efficiency alone leads to a variance $V = 1 - \eta$ of the correlated zones, and therefore we can immediately deduce a lower limit of 10% on the quantum efficiency, in agreement with estimates we have made in the past [23].

A second, less severe but intrinsic imperfection comes about because the momenta of the correlated atoms are not exactly equal and opposite, but have a width determined by the momentum spread within the initial condensates, as confirmed by the finite width of the two-body correlation function in momentum space [17]. Thus it is possible for the two atoms of a correlated pair to end up in zones that are not diametrically opposed. We can study this effect by observing how the variance changes as we change the number of zones N_Z (Fig. 3). The smaller the zones, the more likely that an atom will miss the zone diametrically opposed to that of its partner.

Since we have measured the correlation function for back-to-back momenta, we can model the trend seen in Fig. 3. The back-to-back correlation function was measured to have rms widths of $0.17v_{\mathrm{rec}}$ in the radial (x and y) directions, and $0.02v_{\mathrm{rec}}$ in the axial (z) direction. Neglecting the much smaller axial correlation width, we estimate the probability $P(N_Z)$ that, given an atom hitting one zone, its partner will hit the diametrically opposite one. This probability decreases as N_Z increases, and, taking both quantum efficiency and the geometrical hit probability into account, we expect $V = 1 - \eta P$. The function $V(N_Z)$ is plotted as the solid line in Fig. 3. The approximate agreement of this simple model with the data leads us to conclude that the above two loss mechanisms account very well for the observed variance. We also get a slightly better lower limit on the quantum efficiency, $\eta > 12\%$.

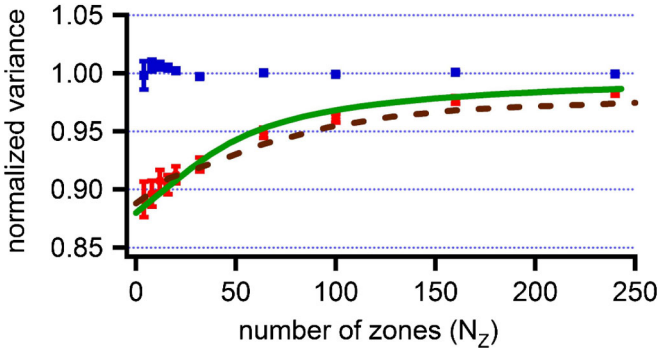

FIG. 3 (color online). Observed variance, as a function of the number of zones into which we cut the halo. Red circles: average over all correlated zones; blue squares: average over all uncorrelated zones. Error bars show the standard deviation of the mean of the variances for a given N_Z. The solid curve is the prediction of the simple model discussed in the text. The dashed curve results from the stochastic Bogoliubov simulation. Both models assume a 12% quantum efficiency.

The situation was also analyzed using a stochastic Bogoliubov simulation as in Ref. [24]. The result for the variance is shown as the dashed curve in Fig. 3. The curve is plotted assuming a detector quantum efficiency of 12% as in the simpler model. The simulation shows the observed trend, but agrees less well with the data than the simple model. The discrepancy arises because the simulation predicts a narrower back-to-back correlation function than was observed in the data, thus resulting in a slower approach to unity for the variance. A finite temperature effect may be at the origin of the difference since the simulation assumes zero temperature. The simulation also neglected mean field repulsion of different spin components, so that such effects could also be responsible. The calculation nevertheless confirms the idea that the lack of perfect correlation in momentum determines most of the variation seen in Fig. 3.

Other known imperfections include the possible contamination of the sphere by atom pairs with one atom in the $m = 0$ state and another in the $m = 1$ state. These pairs contribute a single detected atom without a partner to the halo. We have no independent experimental estimate of the number of such collisions, but they could account for as much as one-half of the observed atoms on the halo. Their presence would mimic a loss in detector quantum efficiency and thus raise our lower limit on η. Spontaneous emission processes act in the same way, but independent measurements indicate that such processes contribute only about 1.5% of the detected atoms on the analyzed halo. As discussed above, the halo centered at $-v_{\mathrm{rec}}$ was more affected by spontaneous emission, though squeezing is still also observed, albeit to a lesser degree. While one might hope to improve the quantum efficiency of the detector, or suppress unwanted scattering events, the stochastic Bogoliubov simulation with $\eta = 1$ predicts a limiting variance $V \approx 0.1$ for a small number of zones. Thus, correcting for the quantum efficiency, the intrinsic squeezing appears to be, at most, -10 dB.

Relative number squeezing is also related to the violation of a classical Cauchy-Schwarz inequality [25,26],

$$\langle N_i N_j \rangle \leq \sqrt{\langle N_i^2 \rangle \langle N_j^2 \rangle}, \tag{2}$$

relating the count rates in two correlated zones i and j. For equal count rates in the two zones, relative number squeezing is strictly equivalent to the violation of the inequality (2). In our experiment the average count rates are not exactly equal, in which case squeezing and Cauchy-Schwarz violation are not equivalent [27]. Nevertheless, we do observe a violation of the inequality (2). More sophisticated inequalities can also be invoked and will be studied in future work.

For purposes of interferometry, one would like to increase count rates and the number of atoms per mode. This could be achieved in a four-wave mixing experiment inside an optical lattice to modify the dispersion relations of the

atoms so as to populate a single pair of modes [28–30]. Such well-defined twin atom beams would permit the realization of experiments such as the celebrated experiment of Hong, Ou, and Mandel [31], or the realization of an interferometer in the spirit of [9–11]. Even more ambitious would be the demonstration of entanglement of the pairs by making Bell-type measurements of the well-separated neutral atoms, in analogy with the measurement made in Ref. [12] using photons.

This work was supported by the French ANR, the IFRAF Institute, and the Euroquam Project CIGMA. G. P. is supported by a European Union Marie Curie IIF Fellowship. P. D. acknowledges the EU Contract No. PERG06-GA-2009-256291. K. K. acknowledges support from the Australian Research Council.

*Present address: Institut Langevin, ESPCI Paris Tech, CNRS, Paris France.

[1] H. A. Bachor and T. C. Ralph, *A Guide to Experiments in Quantum Optics* (Wiley-VCH, Berlin, 2004), 2nd ed.
[2] C.-S. Chuu, F. Schreck, T. P. Meyrath, J. L. Hanssen, G. N. Price, and M. G. Raizen, Phys. Rev. Lett. **95**, 260403 (2005).
[3] S. Whitlock, C. F. Ockeloen, and R. J. C. Spreeuw, Phys. Rev. Lett. **104**, 120402 (2010).
[4] A. Itah, H. Veksler, O. Lahav, A. Blumkin, C. Moreno, C. Gordon, and J. Steinhauer, Phys. Rev. Lett. **104**, 113001 (2010).
[5] J. Estève, C. Gross, A. Weller, S. Giovanazzi, and M. K. Oberthaler, Nature (London) **455**, 1216 (2008).
[6] M. F. Riedel, P. Böhi, Y. Li, T. W. Hänsch, A. Sinatra, and P. Treutlein, Nature (London) **464**, 1170 (2010).
[7] K. Maussang, G. E. Marti, T. Schneider, P. Treutlein, Y. Li, A. Sinatra, R. Long, J. Estève, and J. Reichel, Phys. Rev. Lett. **105**, 080403 (2010).
[8] C. Gross, T. Zibold, E. Nicklas, J. Estève, and M. K. Oberthaler, Nature (London) **464**, 1165 (2010).
[9] P. Bouyer and M. A. Kasevich, Phys. Rev. A **56** R1083 (1997).
[10] J. A. Dunningham, K. Burnett, and S. M. Barnett, Phys. Rev. Lett. **89**, 150401 (2002).
[11] R. A. Campos, C. C. Gerry, and A. Benmoussa, Phys. Rev. A **68**, 023810 (2003).
[12] J. G. Rarity and P. R. Tapster, Phys. Rev. Lett. **64**, 2495 (1990).
[13] M. D. Reid, P. D. Drummond, W. P. Bowen, E. G. Cavalcanti, P. K. Lam, H. A. Bachor, U. L. Andersen, and G. Leuchs, Rev. Mod. Phys. **81**, 1727 (2009).
[14] V. Boyer, A. M. Marino, R. C. Pooser, and P. D. Lett, Science **321**, 544 (2008).
[15] D. C. Burnham and D. L. Weinberg, Phys. Rev. Lett. **25**, 84 (1970).
[16] M. Greiner, C. A. Regal, J. T. Stewart, and D. S. Jin, Phys. Rev. Lett. **94**, 110401 (2005).
[17] A. Perrin, H. Chang, V. Krachmalnicoff, M. Schellekens, D. Boiron, A. Aspect, and C. I. Westbrook, Phys. Rev. Lett. **99**, 150405 (2007).
[18] L. F. Buchmann, G. M. Nikolopoulos, O. Zobay, and P. Lambropoulos, Phys. Rev. A **81**, 031606 (2010).
[19] A. Heidmann, R. J. Horowicz, S. Reynaud, E. Giacobino, C. Fabre, and G. Camy, Phys. Rev. Lett. **59**, 2555 (1987).
[20] M. Schellekens, R. Hoppeler, A. Perrin, J. Viana Gomes, D. Boiron, A. Aspect, and C. I. Westbrook, Science **310**, 648 (2005).
[21] G. B. Partridge, J.-C. Jaskula, M. Bonneau, D. Boiron, and C. I. Westbrook, Phys. Rev. A **81**, 053631 (2010).
[22] C. M. Savage and K. V. Kheruntsyan, Phys. Rev. Lett. **99**, 220404 (2007).
[23] T. Jeltes, J. M. McNamara, W. Hogervorst, W. Vassen, V. Krachmalnicoff, M. Schellekens, A. Perrin, H. Chang, D. Boiron, A. Aspect, and C. I. Westbrook, Nature (London) **445**, 402 (2007).
[24] V. Krachmalnicoff, J.-C. Jaskula, M. Bonneau, V. Leung, G. B. Partridge, D. Boiron, C. I. Westbrook, P. Deuar, P. Ziń, M. Trippenbach, and K. V. Kheruntsyan, Phys. Rev. Lett. **104**, 150402 (2010).
[25] D. F. Walls and G. J. Milburn, *Quantum Optics* (Springer, Berlin, 2008), 2nd ed.
[26] A. Perrin, C. M. Savage, D. Boiron, V. Krachmalnicoff, C. I. Westbrook, and K. V. Kheruntsyan, New J. Phys. **10**, 045021 (2008).
[27] A. M. Marino, V. Boyer, and P. D. Lett, Phys. Rev. Lett. **100**, 233601 (2008).
[28] K. M. Hilligsøe and K. Mølmer, Phys. Rev. A **71**, 041602 (2005).
[29] G. K. Campbell, J. Mun, M. Boyd, E. W. Streed, W. Ketterle, and D. E. Pritchard, Phys. Rev. Lett. **96**, 020406 (2006).
[30] N. Gemelke, E. Sarajlic, Y. Bidel, S. Hong, and S. Chu, Phys. Rev. Lett. **95**, 170404 (2005).
[31] C. K. Hong, Z. Y. Ou, and L. Mandel, Phys. Rev. Lett. **59**, 2044 (1987).